On calculation of stress-strain state of steel closed ropes in extension and twisting
Part 1. Determination of generalized stiffness and deformation coefficients

V. F. Danenko, *Cand. Eng., Associate Prof.[1], e-mail: omd@vstu.ru*
L. M. Gurevich , *Dr. Eng., Associate Prof.[1]*

[1]Volgograd State Technical University, Volgograd, Russia

Comparative analysis of the results of determination of generalized coefficients of stiffness and deformation for closed hoisting rope in extension and twisting was conducted via analytical calculation, using generalized static equations and computer finite element modeling. Computer modeling allows to determine the resulting values of axial force P and torque M in closed rope via summarizing of the values of internal forces and torques in the layers that are laid with different directions. It decreases calculation workability for the rope stress-strain state. It is shown that the results of analytical calculation of generalized stiffness and deformation coefficients in rope twisting differ by 24 % in average with the results of finite element calculation, based on the static equations. The value of rope elasticity module Eк corresponds to the values of elasticity module for closed ropes during the first loading. Analytical calculation provides the values of $E_к$ module exceeding by 6–7 % the average value of elasticity module of closed ropes ($E_к$ = 160 GPa), that is achieved by preliminary elongation (elastic-plastic extension). It was established that analytical calculation of the stiffness coefficient in twisting does not provide the reliable results owing to absence of accounting the difference in directions of laying of rope layers. Coincidence or opposition in directions of laying of rope layers and torque determines respectively extension or compression of rope layer wires in twisting. Untwisting of the external layer, consisting of Z-shape wires, leads to unloading of the layer and gap forming between wires, while this gap exceeds the allowance on wire dimension and promotes violation of rope structural integrity.
Key words: closed hoisting rope, finite element modeling, stress-strain state, wire, rope layer, extension, twisting, force, torque, deformation.
DOI: 10.17580/cisisr.2021.02.04

Introduction

Closed hoisting ropes are related to multi-layer ropes with single laying and they are used as a motive component in lifting and transportation machines and mechanisms. It is known that closed hoisting ropes are used as a rod core for transmission of reciprocating and rotating motion from a surface drive to an operating body of well pump in oil production from wells [1, 2].

Closed ropes are often failing to operate owing to structure violation, such as buckling, lamination, unlocking and destruction of external Z-shape wires etc. [2–6]. To provide reliable and safe rope operation, it is necessary to have trustworthy methods for determination of stress-strain state (SSS) of role elements (wires and layers). The main approaches to theoretical SSS investigation for rope elements were discussed in the works [3, 4, 7–10].

The paper [7] attract attention to the techniques providing higher calculation precision and maximal approximation to construction of the real rope. These techniques are based on the following ideas:

a) discrete model where rope is presented as a complicated and statically undefined rod system that can be subjected to calculation by the methods of building mechanics [3];

b) the theory of fiber composites and solution of the Saint-Venant problem for a cylinder with screw anisotropy [8].

The mathematical model, where each rope layer is considered from the point of view of energetic approach as anisotropic cylinder shell equivalent with its elastic properties, while a rope in general is considered as the system of cylinder shells inserted inside each other and mutually contacting due to contact pressure and friction, is suggested in the works [11, 12].

Independently of the used techniques, the expressions for determination of force parameters in cross section of rope elements during joint extension and rotation are described as the system including two equations [3]:

$$\begin{aligned} P &= A \cdot \varepsilon + C \cdot \theta \\ M &= C \cdot \varepsilon + B \cdot \theta \end{aligned}, \qquad (1)$$

where P — axial force; M — torque; ε and θ — relative deformations of elongation and twisting; A, B and C — generalized stiffness coefficients.

Rope stiffness parameters have influence on their structural integrity and depend on geometric parameters and stiffness of rope elements. Differences in approaches within the rope theory lead to different analytical expressions for determination of generalized stiffness coefficients [7].

According to the technique of M. F. Glushko [3],

$$A = \sum_{i=1}^{n} A_i = \sum_{i=1}^{n} \left[\begin{array}{l} EF_i \cos^3\alpha_i + EI_i \frac{\sin^4\alpha_i}{r_i^2} \times \\ \times \cos^3\alpha_i + GI_{\rho i} \frac{\sin^6\alpha_i}{r_i^2} \cos^2\alpha_i \end{array} \right] \quad (2)$$

$$C = \sum_{i=1}^{n} C_i = \sum_{i=1}^{n} \left[\begin{array}{l} EF_i r_i \cos^2\alpha_i \sin\alpha_i + GI_{\rho i} \frac{\cos^4\alpha_i}{r_i} \times \\ \times \sin^3\alpha_i - EI_i (1 + \cos^2\alpha_i) \frac{\cos^2\alpha_i}{r_i} \sin^3\alpha_i \end{array} \right] \quad (3)$$

$$B = \sum_{i=1}^{n} B_i = \sum_{i=1}^{n} \left[\begin{array}{l} EF_i r_i^2 \cos\alpha_i \sin^2\alpha_i + GI_{\rho i} \cos^7\alpha_i + \\ + EI_i (1 + \cos^2\alpha_i)^2 \sin^2\alpha_i \cos\alpha_i \end{array} \right] \quad (4)$$

According to the technique of I. P. Getman and Yu. A. Ustinov [8],

$$A = \pi k_1 a^2 E \left[1 - \left(1 + \frac{\nu}{2} \right) \sin^2\alpha \right] \quad (5)$$

$$C = \pi k_1 a^3 E \cdot tg\alpha \frac{\left[1 - \left(\frac{4}{3} + \nu \right) \sin^2\alpha \right]}{2} \quad (6)$$

$$B = \pi k_1 a^4 E \cdot tg^2\alpha \frac{\left[1 - \left(\frac{3}{2} + \frac{3\nu}{4} \right) \sin^2\alpha \right]}{3} \quad (7)$$

where E and G – modules of elasticity and shift of wire material; F_i – square of cross section of layer wires; I_i and $I_{\rho i}$ – axial and polar cross section inertial moments; α_i — laying layer angle; r_i – average layer radius; k_1 – relation of summarized square of wires cross sections ΣF_i and square of rope cross section as a round cylinder F_K; a – rope radius as a round cylinder; ν – Poisson coefficient for wires material; α – laying angle for external layer wires.

Solutions of the equations (1) relating to deformations ε and θ are presented as [3]:

$$\varepsilon = \frac{B}{\Delta} P - \frac{C}{\Delta} \cdot M; \quad \theta = -\frac{C}{\Delta} \cdot P + \frac{A}{\Delta} M \quad (8)$$

where $\Delta = A \cdot B - C^2$.

The existing calculation methods can't be used unconditionally for SSS determination of steel ropes, e. g. because the techniques [3, 8] don't take into account friction forces and contact interaction between the rope elements.

Computer-aided simulation of ropes SSS based on the finite element modeling (FEM) using different software products can be considered as an efficient tool for increase of workability during operation of multi-layer ropes [5, 6, 10, 13–15]. This tool does not give up the experimental and analytical methods. The number of researches on computer-aided simulation of closed ropes SSS is restricted [5, 16].

Comparison of SSS calculation results for closed rope during extension and twisting via conventional algorithms and computer-aided simulation methods is the aim of this work.

Materials and methods of investigations

Analysis of a closed rope SSS during axial extension and twisting was conducted via FEM method using licensed software package SIMULIA/Abaqus, allowing to obtain the results with required accuracy and productivity [6, 17, 18]. The cross section of simulating closed rope is shown on the Fig. 1. The core 1 of 1 + 7 + 7/7 + 14 construction is presented by the rope with ordinary laying from round wires with axes having shape of screw lines. These wires are laid with three layers with the same pace around the central straight wire.

Laying direction of the external layer 6 from Z-shaped wires and of the layer 4 from round wires (positions 4 and 2 on the **Fig. 1**) was considered as right (positive), while laying direction of the alternating round and H-shaped wires and the core (positions 3 and 1 on the Fig. 1) was considered as left (negative). If laying directions are different, the layers from round wires contact in a points, while the contact of shaped section wires can be considered as linear one [3].

Parameters and dimensions of 20.5 mm diameter (d) rope elements that were used during simulation and the same as those presented in the researches [5, 18]. The length simulating rope sample l_o = 130 mm, elasticity module of wire material $E = 2 \cdot 10^5$ MPa, friction coefficient $\mu = 0.1$.

The edges of wires layers at the rear end of simulating rope were firmly connected with the edge surface of a movable auxiliary hard disk, and at the front end – with coaxially located fixed hard internal disk (connected with the core 1 + 7 + 7/7 + 14 — position 1 on the Fig. 1) and rings (connected with the layers 4–6 — positions 2–4 on the Fig. 1).

The scheme of analytical SSS calculation of the spiral rope includes the following steps [3]: determination of the generalized rope stiffness coefficients (A, B and C) according to the equations (2–4) и (5–7); calculation of rope deformation ε and θ with preset external load as axial force P and torque M, according to the equations (8); evaluation of distribution of force and torque load along the rope layers and internal forces in transversal cross sections of ropes; determination of stresses occurring in transversal cross sections of rope wires.

Definition of SSS parameters for the closed rope elements during simulation was conducted for the following loading variants:

1. Pure extension – the model for transition of longitudinal force from the surface drive to the well pump ($\varepsilon \neq 0$; $\theta = 0$). The rope sample was extended with 4 mm/s speed up to reaching the axial force value P ~ 120 kN. These parameters were chosen taking into account the load capacity 80 kN and rope mass with 1,500 m length, due to axial transition of a movable hard disk (excluding possibility of its rotation).

2. Pure twisting — the model for transition of rotating motion from the surface drive to the well pump ($\varepsilon^\circ = 0$; $\theta \neq 0$). Twisting of the rope sample was conducted by external torque *M*, due to turning of a movable hard disk (without any axial transitions), with speed 36 grad/s for the maximal turning angle $\varphi \approx 20^\circ$.

The result of SSS simulation for the closed rope elements during pure extension and twisting allowed to determine generalized stiffness coefficients *A, B* and *C*, and then to determine the values of linear ε and angular θ deformations for resulting values of force factors, according to the equations (8). The resulting values of force *P* and torque *M* in the rope were determined by summarizing of the values of external forces and torques in the rope layers [5].

Table 1. **Results of calculation of generalized coefficients and rope deformations**

Line No.	Technique	Generalized coefficients			Relative elongation (pure extension) ε, %	Relative angle of twisting (pure twisting) θ, rad/m
		A, MN	C, kN·m	B, N·m²		
1	M. F. Glushko [3]	46.26	34.42	1653.56	0.259	–0.12/0.39*
2	I. P. Getman, Yu. A. Ustinov [8]	45.80	75.77	178.07	0.262	–1.08/3.65*
3	Simulation	37.15	21.18	71.75/ 242.76*	0.323	–2.68/2.68*

* numerator — untwisting, denominator — twisting of a rope sample

Results and discussion

The values of generalized stiffness coefficients of the examined rope were calculated according to the equations (2–4) and (5–7) and presented in the **Table 1** (lines 1 and 2). While the values of coefficients *A* differ slightly, the values of coefficients *C* differ by 2.2 times, what is connected with accounting of the laying angle sign of rope layers during calculation of the coefficient *C* according to the equation (3) with uneven degree of the laying angle sine. Difference between the obtain values of the coefficient *B* by the order is connected with no accounting of the laying angle sign of rope layers during calculation according to the equation (4).

Let's compare the results of analytical calculation of the stiffness generalized coefficients with the results obtained via use of computer simulation method.

For the case of pure extension we shall obtain from the equations (1)

$$P = A \cdot \varepsilon, \qquad M = C \cdot \varepsilon = C \cdot \frac{P}{A}. \tag{9}$$

The results of rope extension simulation testify [5] that general elongation of a rope sample makes $\varepsilon = 0.563$ % of initial length, while constructive (residual) elongation is $\varepsilon_{res} = 0.24$ %, when the force *P* achieves ~ 120 kN. Residual elongation is observed owing to running-in of laid wires during the first loading [19], what is confirmed experimentally [10] as well as with the features of forces distribution in a rope and its layers on the initial section of the extension curve (**Fig. 2**).

The lower initial values of extension forces in the external layers 5 and 6 (curves 3 and 4) are connected with retarding of creation of supporting surfaces for counteraction to circular compression loads due to essential value of initial circular gap between wires in layers [18]. Exclusion of

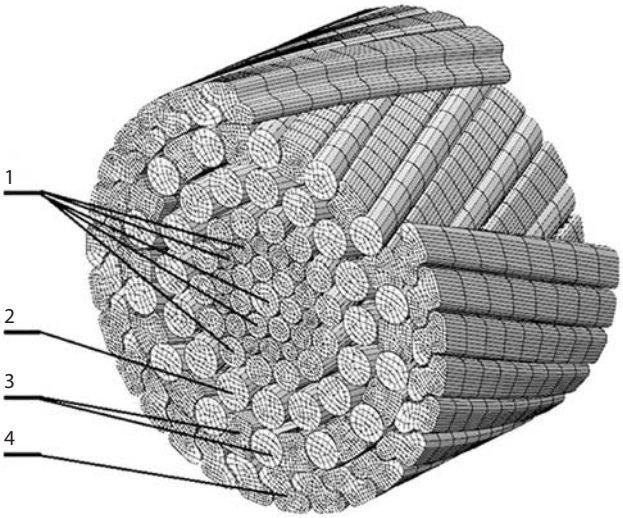

Fig. 1. Cross section of closed rope (part of the external layer is conditionally deleted): 1 – core (round wires); 2 – layer 4 (round wires); 3 – layer 5 (round / H-shaped wires); 4 – layer 6 (Z-shaped wires)

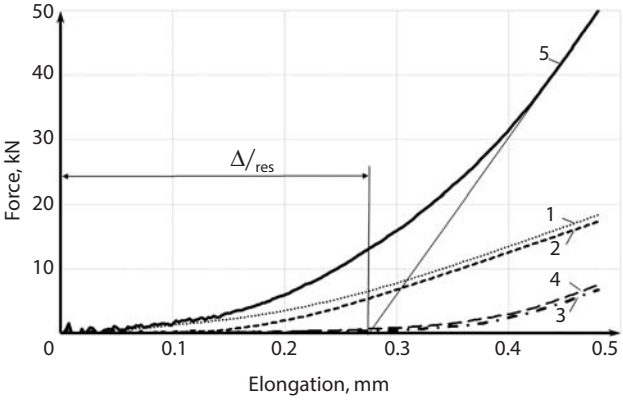

Fig. 2. Forming of residual elongation during tope extension: 1 — core; 2 — layer 4; 3 — layer 5; 4 — layer 6; 5 — rope

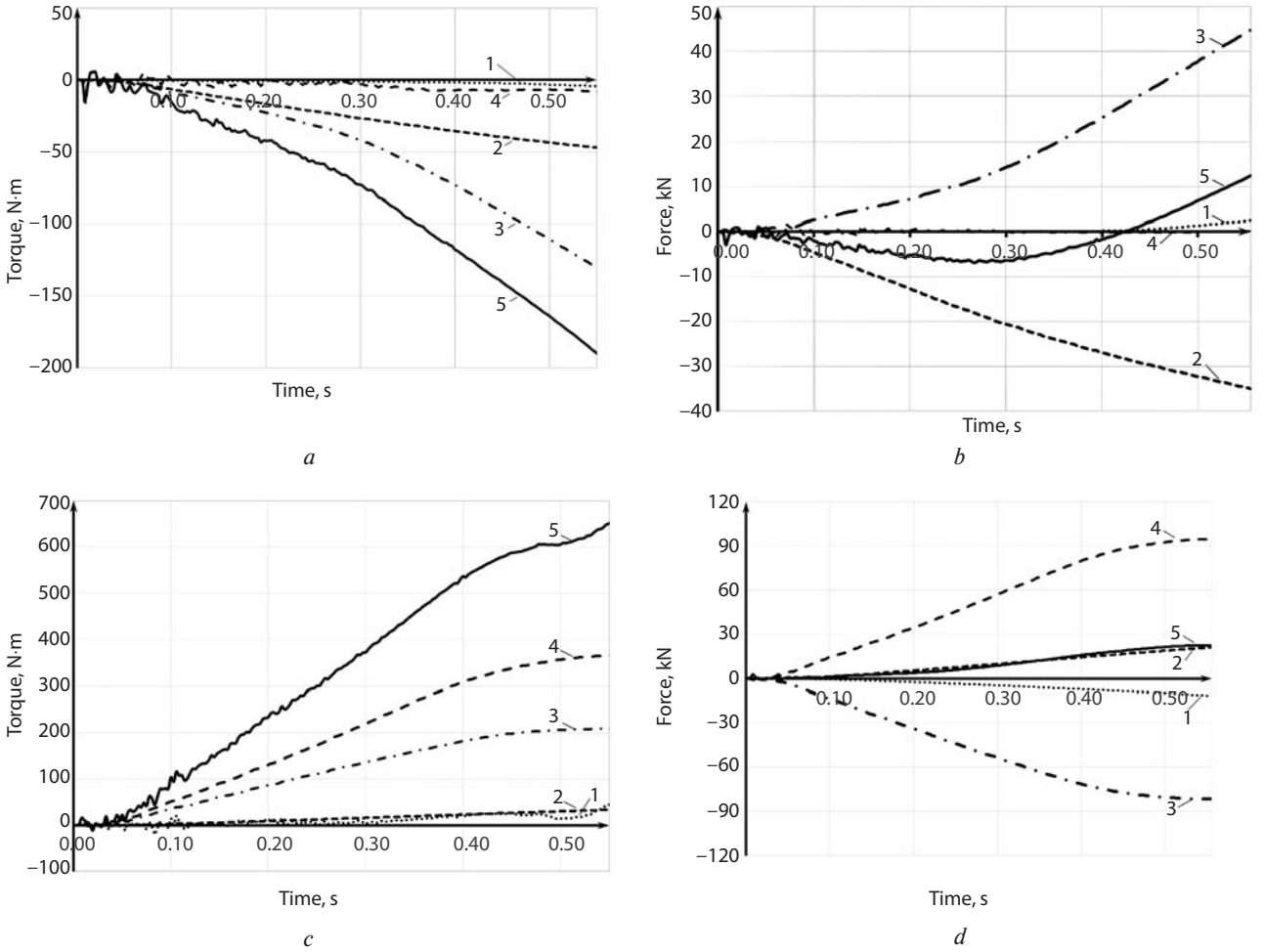

a *b* *c* *d*

Fig. 3. Distribution of the torques and axial forces in the rope and its layers during pure twisting – for untwisting (*a, b*) and twisting (*c, d*): 1 — core; 2 — layer 4; 3 — layer 5; 4 — layer 6; 5 — rope

residual elongation ε_{res} provides the value of elastic elongation of a rope sample $\varepsilon = 0.323$ % from the initial length. Then the stiffness coefficient for elongation makes

$$A = P / \varepsilon = \frac{120}{0.323} 10^5 = 37.15 MN \quad \text{(see the Table 1).}$$

The values of stiffness coefficient *A* and, respectively, relative elongation ε during simulation of pure rope extension differ by 24 % in average from the calculation results according to the techniques [3] and [8]. In this case, the rope elasticity module $E_к = A/F_{m.ch.} = 137.6$ GPa, where $F_{m.ch} = 270$ mm^2 is metallic square of rope cross section. The conducted tests on extension of the examined rope at the universal testing hydraulic horizontal machine LabTest 6.2000H.7 (Czech Republic) displayed [20], that the value of rope elasticity module makes $E_к = 137.0$ GPa. The results of module $E_к$ determination, which were obtained during simulation, are practically corresponded with the experimental data. In the existing practice, the rope elasticity module $E_к$ is connected with the elasticity module of wires *E* via the relationship $E_к = aE$, where a<1. According to I. Stefan, $a = 0.65$ for closed ropes [19]. Then $E_к = 0.65 \cdot 210 = 136.5$ GPa, what, corresponds to the values $E_к = 130 \div 140$ GPa for spiral ropes during the first loading [19]. At the same time, assessment of the rope elasticity module according to the techniques [3] and [8] and based on the values of the coefficient A presented in the Table 1, displays the value $E_к \approx 170$ GPa, which exceeds the average value $E_к = 160$ GPa for closed rope after preliminary elongation [21].

The resulting torque during extension is equalizing by the fixing torque, and it makes $M = 68.4$ N·m for $P = 120$ kN [5]. The value of influence coefficient $C = M/\varepsilon = 21.18$ kN·m (Table 1) is found from the equation (9). Comparison of the torque values $M = 90.8$ N·m (the technique [3]) and $M = 198.5$ N·m (the technique [8]), which were calculated via the equation (9), testifies about exceeding by 1.33 and 2.9 times respectively for the torque value obtained during extension simulation. Deviation between these values is explained by different influence coefficient values *C* (see the Table 1), which were calculated according to the equations (3) and (6). It is possible to minimize the resulting torque arising during extension and, respectively, the influence coefficient C by choosing directions and laying angles of rope layers. The ropes meeting the requirements of the condition C→0 are named as equalized ropes [3].

For the case of pure twisting, we can get the following equations from the equation (1):

$$P = C \cdot \theta, \qquad M = B \cdot \theta. \tag{10}$$

For the case of untwisting the rope sample by external negative torque M (Fig. 3*a*), the wires of layer 5 are compacted as a result of twisting and lead to decrease of the axial layer length. Fixing of rope sample ends as well as untwisting layers 6 and 4 obstruct this process. As a result, extending and compressing forces arise in the layers 5 and 4 respectively (see the curves 3 and 2 on the Fig. 3*b*). The external layer 6 and rope sample core are practically not subjected to loading during untwisting (see the curves 4 and 1 on the Fig. 3*b*).

In the case of rope sample twisting by positive external torque M (see Fig. 3*c*), the above-described behaviour of layers changes to alternating one. The wires of layers 6 and 4 are compacted as a result of twisting and lead to decrease the axial length of layers and the rope sample in general. Fixing of rope sample ends as well as untwisting layer 5 and core obstruct to this process. As a result, the extending forces arise in the layers 4 and 6 (curves 2 and 4 on the Fig. 3*d*), while in the core and layer 5 arise compressing forces (curves 1 and 3 on the Fig. 3*d*).

The results of rope untwisting simulation testify that the resulting torque makes $M = -192.3$ N·m (curve 5 on the Fig. 3*a*) for the boundary value of cross section turning angle $\varphi \approx 20°$. The stiffness coefficient during twisting from the equation (10) is $B = M/\theta = 192.3/2.68 = 71.75$ N·m^2. For the case of rope twisting, the boundary value of the resulting torque is $M = 650.6$ N·m (curve 5 on the Fig. 3*c*). The stiffness coefficient makes $B = 650.6/2.68 = 242.76$ N·m^2. The linear type of the curves 5 (see the Fig. 3*a* and *b*) confirms correctness of determination of stiffness coefficients in the examined range of cross section turning angles. Calculated values of the coefficient B are presented in the Table 1 (line 3).

Deviation between the calculated values of relative twisting angle θ according to the techniques [3] and [8] and the angle $\theta = \pm 2{,}68$ rad/m which was preset during simulation is connected with difference of the values of stiffness coefficients B during twisting (see Table 1), calculated according to the equations (4) and (7).

The results of simulation show that rope twisting leads to non-uniform distribution of forces in the layers. When directions of a layer laying and torque M coincide, layer wires are in the extended state. Alternatively, if directions of a layer laying and torque M are contrary, wires are unwinding and are in the compressed state. Increase of the external layer diameter during rope untwisting [22] is like loss of stability ("opening") of closed rope under the effect of compressing loads [2, 23]. The calculation display that achieving of the untwisting angle $\varphi \approx 20°$ leads to the gap between external layer wires as large as 0.085 mm, what exceeds the allowance for wire dimension $\Delta = \pm 0.08$ mm according to the GOST P 58134-2018. Choice of the gap value between the wires in external layers and assessment of the contact stresses between adjacent wires using the method of finite element modeling allow to provide saving of structural rope operating integrity during designing of closed ropes.

Conclusions

1. The results of extension simulation of closed rope in elastic area show that the obtained value of the rope elasticity module $E_к = 137.6$ GPa corresponds with the values of elasticity module of closed ropes $E_к = 130 \div 140$ GPa during the first loading. The values of elasticity module obtained via analytical calculation are excessive and exceed by 6–7 % the average value of elasticity module for closed ropes $E_к = 160$ GPa which was achieved after preliminary elongation (elastic-plastic extension).

2. The methods of analytical calculation for the stiffness coefficient B during twisting don't provide the trustworthy result, because they don't take into account the differences in laying directions of rope layers. The results of finite element calculation show that rope twisting increases non-uniformity of distribution of axial forces in the rope layers in comparison with extension. Difference in laying direction of the layers leads to simultaneous existence of extending and compressing wires of neighbor layers in twisting, what can finalize in appearance of the rope structural defects. It was established that untwisting of the external layer during turning of the cross section by the angle $\varphi \approx 20°$ leads to gap forming between Z-shape wires, which exceeds the allowance for wire dimension.

REFERENCES

1. Ivanovskiy V. N., Sabirov A. A., Degovtsov A. V., Pekin S. S. Rope pump rod. Patent 2527275 RU. Bill. No. 24. Announced 24.06.2013. Published 27.08.2014.
2. Ivanovskiy V. N., Sabirov A. A., Mazein I. I. et al. Efficiency rise of oil wells operation with side holes of small diameter. *Neftegaz.ru*. 2019. No. 6. pp. 62–69.
3. Glushko M. F. Steel lifting ropes. Kiev: Tekhnika. 1966. 328 p.
4. Khalfin M. N., Ivanov B. F., Kharkovskiy E. V. Determination of the strength reserve factor for a track rope with buckling account. *Izvestiya Tulskogo gosudarstvennogo universiteta. Tekhnichexkie nauki*. 2018. No. 1. pp. 122–126.
5. Danenko V. F., Gurevich L. M. Simulation of stress-strain state of closed rope during stretching and twisting. *Deformatsiya i razrushenie materialov*. 2021. No. 1. pp. 2–9.
6. Song B., Wang H., Cui W., Liu H., Yang T. Distributions of stress and deformation in a braided wire rope subjected to torsional loading. *The Journal of Strain Analysis for Engineering Design*. 2018. Vol. 54. No. 1. pp. 3–12. DOI: 10.1177/0309324718800814.
7. Kalentyev E. A., Tarasov V. V. Numerical analysis of the stress-strain state of a rope thread with linear touch during extension and twisting. *Vychislitelnaya mekhanika sploshnykh sred*. 2010. Vol. 3. No. 4. pp. 16–28.
8. Getman I. P., Ustinov Yu. A. About the methods of ropes calculation. The problem of extension-twisting. *Prikladnaya matematika i mekhanika*. 2008. Vol. 72. Iss. 1. pp. 81–90.
9. Polyakov S. V. Study of the lifting rope with appeared variations of geometrical parameters and mechanical properties of screw elements. *Nauchno-tekhnicheskiy vestnik Bryanskogo gosudarstvennogo universiteta*. 2019. No. 2. pp. 257–264.
10. Liu H., Wang H., Song B., Han X., Han B., Lin J. Modeling of braided wire ropes under tension and torsional loads. *The Journal of Strain Analysis for Engineering Design*. 2020. Vol. 56. No. 4. pp. 216–224. DOI: 10.1177/0309324720958257.
11. Danilin A. N., Ryzhov S. V., Tsvetkov Yu. L., Shalashilin V. I. A wire model for overhead transmission line. *Mekhanika kompozitsionnykh materialov i konstruktsiy*. 2005. Vol. 11. No. 4. pp. 564–572.
12. Anosov V. Yu., Danilin A. N., Kurdyumov N. N. On stiffness of spiral-type wire constructions. *Trudy MAI*. 2015. No. 80. http://www.mai.ru/science/trudy/published.php?ID=56958.

13. Tarasov V. V., Kalentyev E. A., Novikov V. N. Steel ropes. Calculation of constructions and assessment of operating properties. *Mekhanika i fisiko-khimiya geterogennykh sred, nanosistem i novykh materialov.* 2015. pp. 237–259.
14. Jun M. A., Shi-rong G. E. , De-kun Zhang. Distribution of wire deformation within strands of wire ropes. *Journal of China University of Mining & Technology*. 2008. Vol. 18. No. 3. pp. 475–478.
15. Fontanari V., Benedetti M., Monelli B. D. Elasto-plastic behavior of a Warrington-Seale rope: Experimental analysis and finite element modeling. *Engineering Structures*. 2015. Vol. 82. pp. 113–120.
16. Raoof M., Kraincanic I. Prediction of coupled axial/torsional stiffness coefficients of locked-coil ropes. *Computers and Structures*. 1998. Vol. 69. pp. 305–319.
17. Antonova O. V., Nemov A. S., Voinov I. B., Goncharov P. S., Borovkov A. I. Finite element analysis of ropes. Comparison of Abaqus, LSDYNA, MSC. MARC software systems. *XXXVI week of science in St. Petersburg State Polytechnic University: Proceedings of the All-Russian inter-university scientific-technical conference of students and post-graduates. St. Petersburg, November 26 – December 1). St. Petersburg.* Izdatelstvo SPbGPU. 2009. http://elib.spbstu.ru/dl/007906.pdf.
18. Danenko V. F., Gurevich L. M. Simulation of extension effect on structural integrity of lifting ropes with closed construction. *Materialovedenie*. 2020. No. 2. pp. 43–48.
19. Bukshtein M. A. Production and use of steel ropes. Moscow: Metallurgiya. 1973. 360 p.
20. Malinovskiy V. A. Steel ropes. Part 1. Several technological, calculating and designing problems. Odessa. Astroprint. 2001. 188 p.
21. Danenko V. F., Gurevich L. M., Myazina I. R. Radial transition of lifting ropes elements with closed construction during their joint extension and twisting. *Izvestiya VolgGTU: nauchnyi zhurnal. The Series "Problemy materialovedeniya, svarki i prochnosti v mashinostroenii"* 2019. Vol. 233. No. 10. pp. 68–74.
22. Aliev Sh. A., Zinovyev A. V., Degovtsov A. V., Pekin A. S. Studies of strength properties of ropes with different constructions used as rope rods under effect of compressing loads. *Territoriya NEFTEGAZ.* 2019. No. 6. pp. 52–57.